

EGU2020-3169: Properties of OH roto-vibrational level populations in the Earth's mesopause region

Stefan Noll^{1,2}, Holger Winkler³, Oleg Goussev², and Bastian Proxauf⁴

¹Institut für Physik, Universität Augsburg, Augsburg, Germany

²DFD, DLR Oberpfaffenhofen, Weßling, Germany

³Institut für Umweltphysik, Universität Bremen, Bremen, Germany

⁴Max-Planck-Institut für Sonnensystemforschung, Göttingen, Germany

Content of display:

Summary with five figures

Full study is published in ACP:

<https://www.atmos-chem-phys.net/20/5269/2020/>

<https://doi.org/10.5194/acp-20-5269-2020>

Summary

- High-resolution average sky spectrum between 570 and 1,040 nm from the VLT/UVES echelle spectrograph at Cerro Paranal, Chile:
 - about 1,000 individual line measurements in 16 OH bands
- Investigation of OH level populations for six sets of Einstein-A coefficients (Fig. 1):
 - Varying (and often large) discrepancies for comparisons between bands as well as branches; bad performance of all sets for Q branches and Λ doublets
 - The most promising set is Brooke et al. (2016) based on number of lines and comparisons of bands and branches.
 - Empirical improvement of Brooke et al. (2016) Einstein-A coefficients based on measured population differences (Fig. 2)
- Characterisation of OH roto-vibrational level population distributions:
 - Combination of cold and hot population for each vibrational level (Fig. 3)
 - Good fit with simple two-temperature model (Fig. 3), which also offers a robust estimate of non-LTE contributions to rotational temperatures (Fig. 4).
 - Cold and hot populations vary differently for changing OH layer heights (Fig. 5).

Impact of Einstein-A coefficients on OH level population

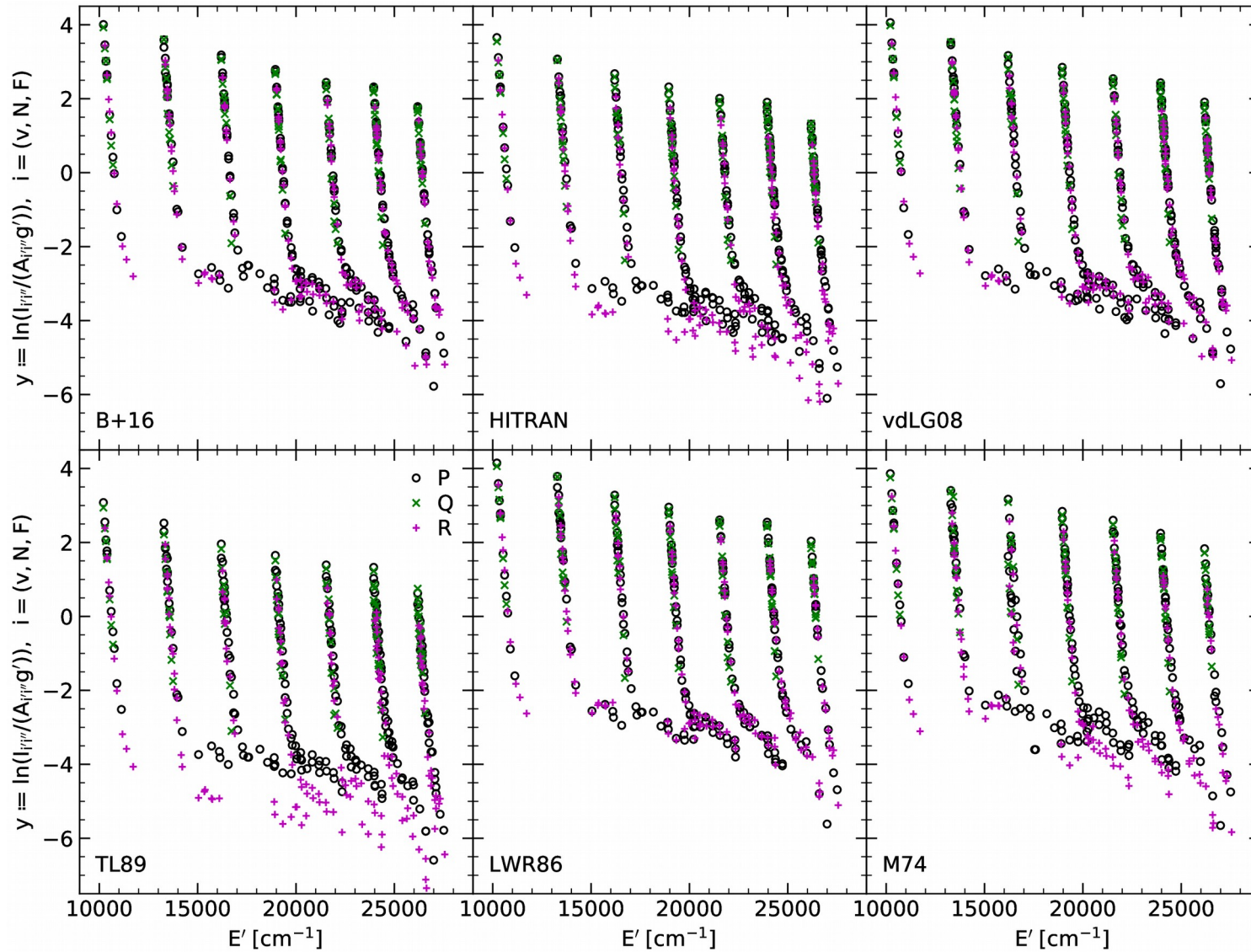


Fig. 1: OH level populations from up to 544 measured Λ doublets for six different sets of Einstein A-coefficients: Brooke et al. (2016) (B+16), HITRAN (Rothman et al. 2013), van der Loo and Groenenboom (2008) (vdLG08), Turnbull and Lowe (1989) (TL89), Langhoff et al. (1986) (LWR86), and Mies (1974) (M74). For more details, see Fig. 5 in the ACP paper.

Correction of Brooke et al. (2016) A-coefficients

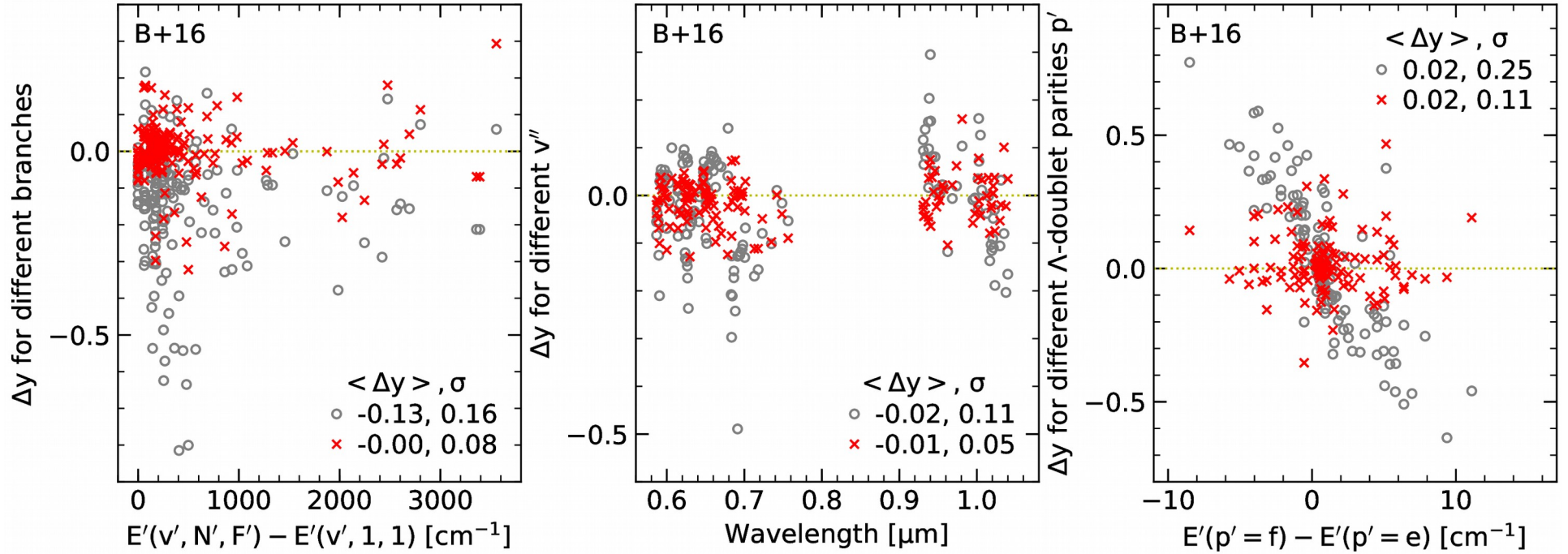


Fig. 2: Natural logarithm of OH level population ratios Δy for lines only differing in the branch as a function of level energy (**left**), only differing in the vibrational level of the lower state v'' as a function of line wavelength (**middle**), and only differing in the Λ -doublet parity as a function of the energy gap (**right**). Circles show the results for the original B+16 A-coefficients, whereas crosses indicate those related to the empirically corrected B+16 A-coefficients. For more details, see Fig. 11 in the ACP paper.

Fit of rotational level populations

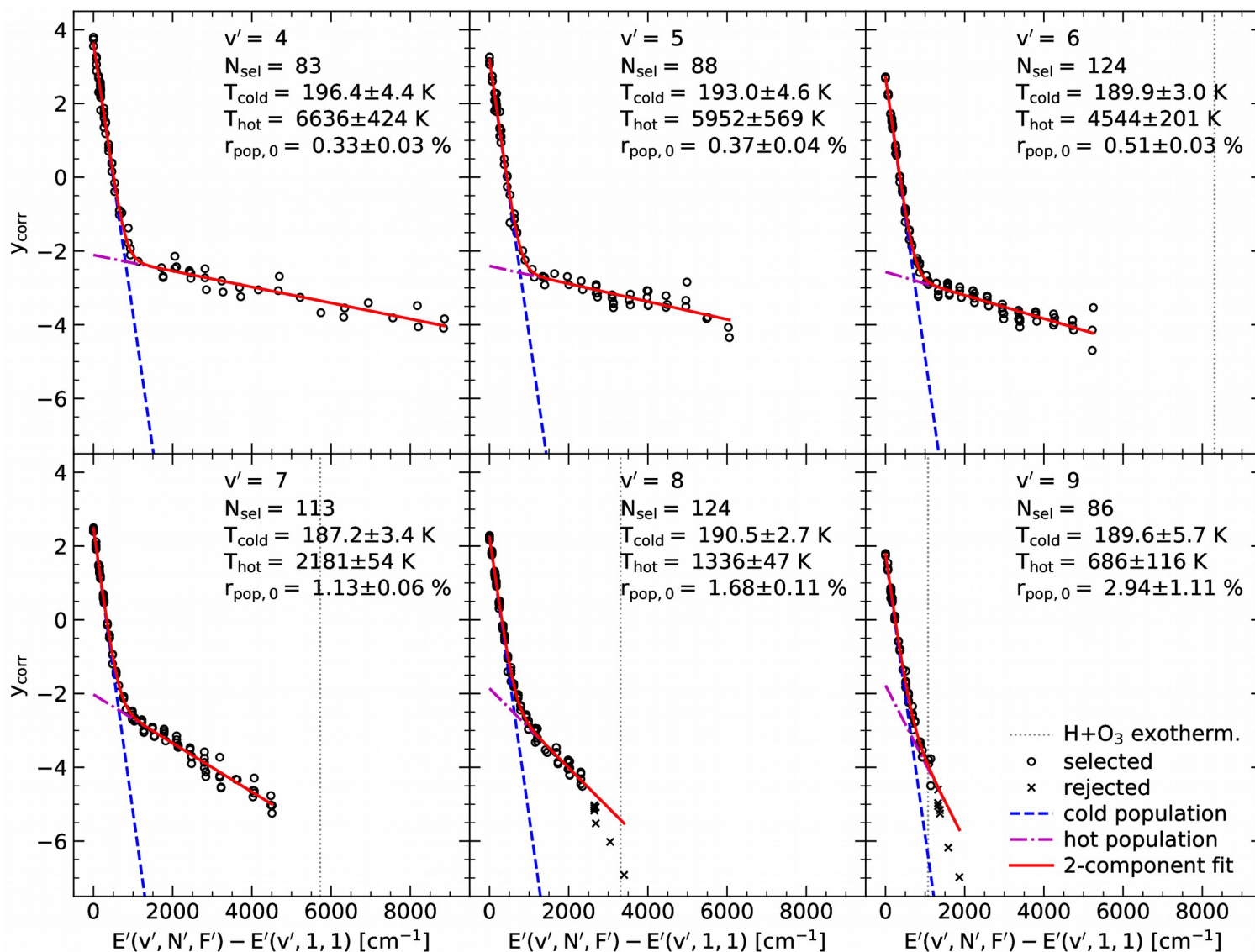


Fig. 3: OH level populations calculated with the corrected B+16 A-coefficients for different upper vibrational levels v' as a function of the level energy. The populations can be fitted well with a two-temperature model consisting of a cold and a hot component. For more details, see Fig. 12 in the ACP paper.

Non-LTE contributions to rotational temperatures

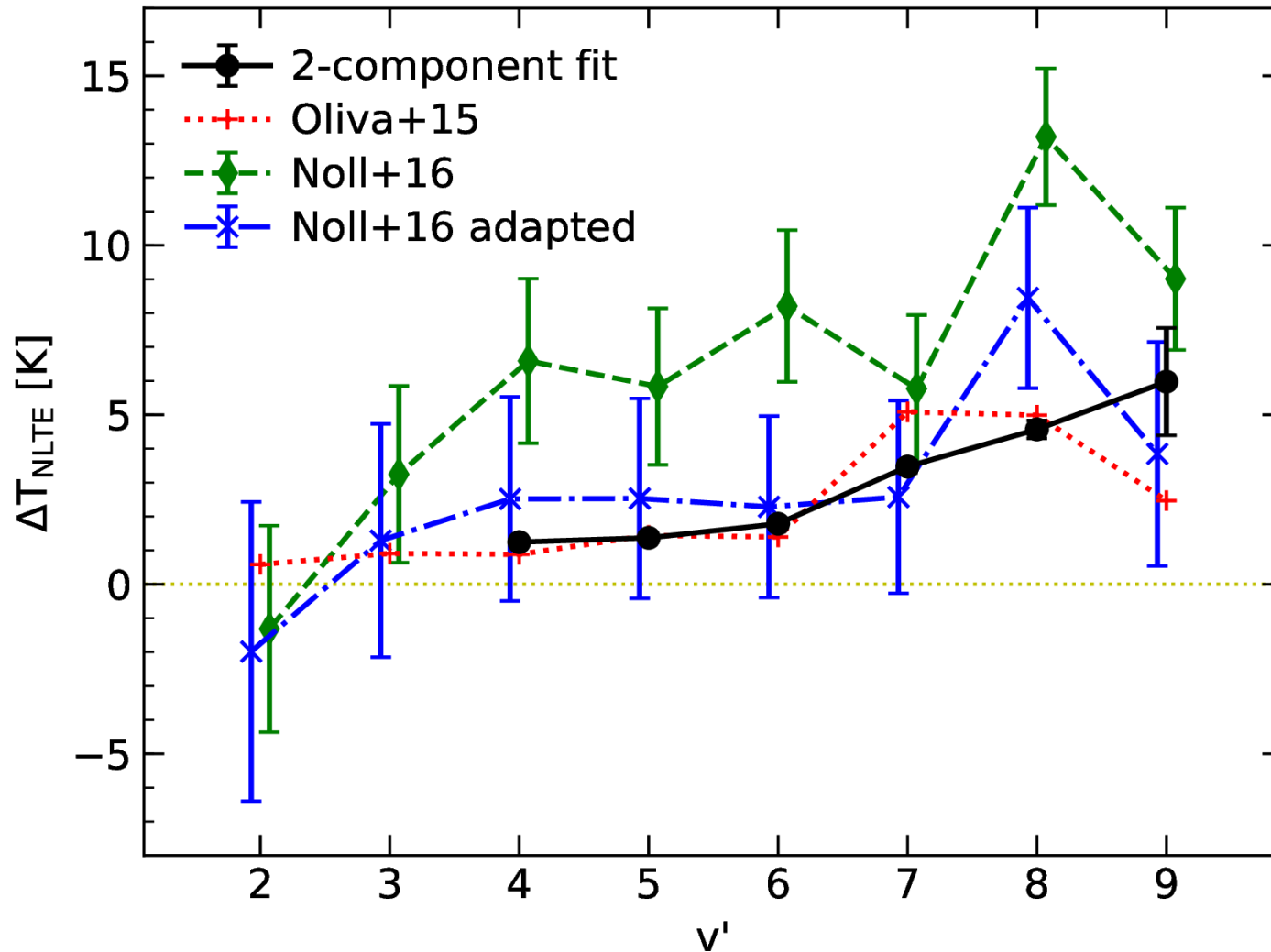


Fig. 4: Non-LTE contributions to rotational temperatures derived from the first three P_1 -branch lines of a vibrational level v' based on two-component fits of the derived OH level populations (circles and solid lines). Moreover, the plot shows ΔT_{NLTE} for the two-component fits of Oliva et al. (2015), the analysis of Noll et al. (2016), and its modification especially with respect to the A-coefficients used. For more details, see Fig. 13 in the ACP paper.

Dependence of OH level populations on layer height

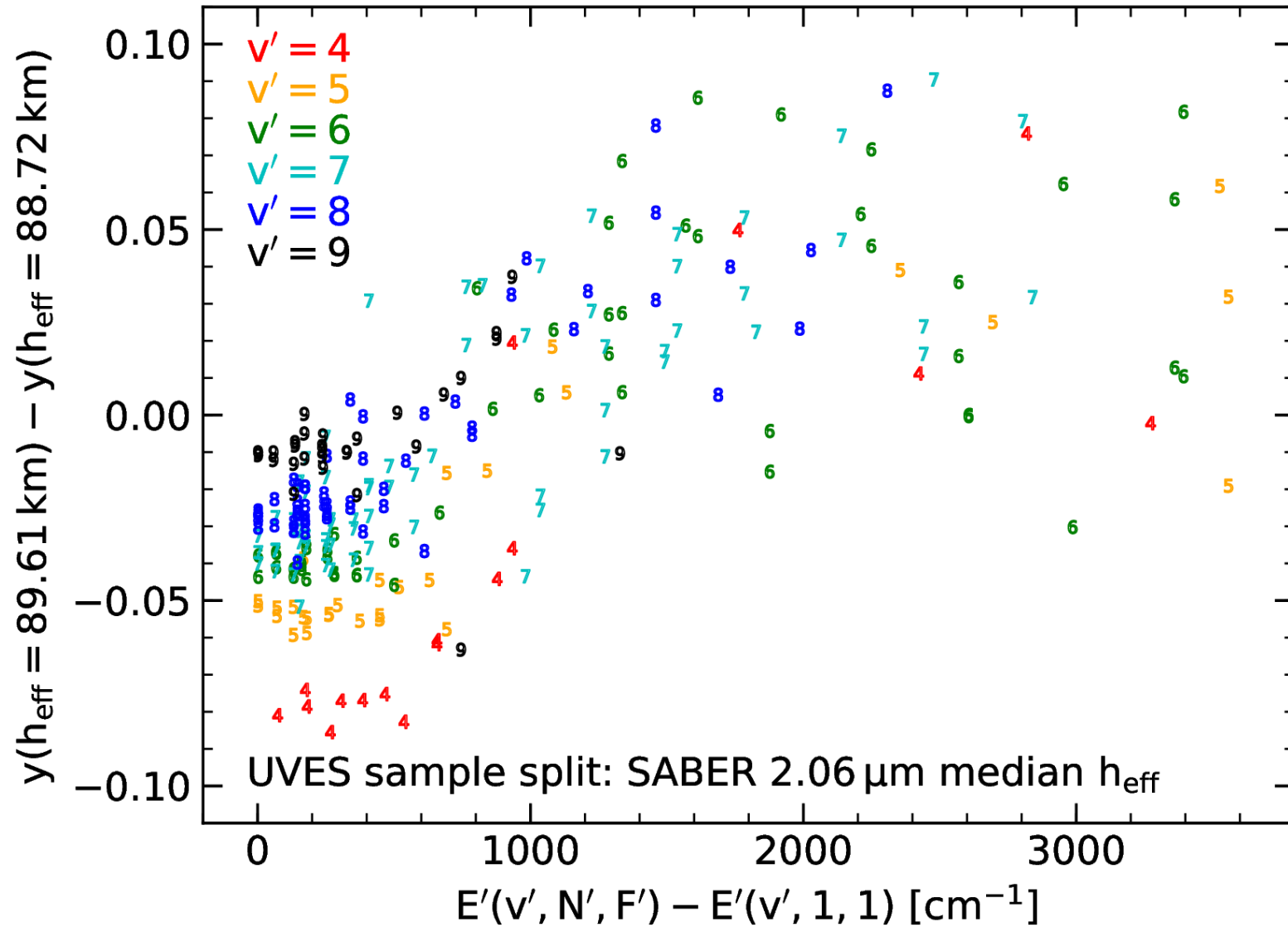


Fig. 5: Difference in logarithmic OH level populations for UVES mean spectra based on equally sized subsamples of high and low effective emission height h_{eff} as a function of the level energy. The coloured numbers indicate the related upper vibrational level v' . For more details, see Fig. 14 in the ACP paper.